

Supporting Information: Topological-Defect-Induced Superstructures on Graphite Surface

Zi-lin Ruan(阮子林), Zhen-liang Hao(郝振亮), Hui Zhang(张辉), Shi-jie Sun(孙诗杰),
Yong Zhang(张永), Wei Xiong(熊玮), Xing-yue Wang(王兴悦), Jian-chen Lu(卢建臣)*,
and Jin-ming Cai(蔡金明)

Faculty of Materials Science and Engineering, Kunming University of Science and Technology,
Kunming 650000, China

* Supported by the National Natural Science Foundation of China (11674136, 61901200), the Thousand Talents Plan-The Recruitment Program for Young Professionals (1097816002), Yunnan Province for Recruiting High-Caliber Technological Talents (1097816002), reserve talents for Yunnan young and middle aged academic and technical leaders (2017HB010), the Yunnan Province Science and Technology Plan Project (Grant No. 2019FD041), the China Postdoctoral Science Foundation and the Yunnan Province Postdoctoral Science Foundation..

*Corresponding author. Email: jclu@kust.edu.cn.

1. Experimental details

All STM/S experiments were performed by using an ultrahigh vacuum low-temperature scanning tunneling microscopy (LT-STM) system (Scienta Omicron) with a base pressure better than 1×10^{-10} mbar. Fresh HOPG surface is cleaved using adhesive tape at atmosphere and transferred into load lock chamber immediately to avoid impurity adsorption. After degassed at 400°C overnight, the sample is transfer to STM. All STM/S measurements were performed at 4.2 K with a Pt/Ir tip, all topographic images were acquired in constant-current mode. For STS characterization, the dI/dV measurements have been performed with a lock-in amplifier (Zurich Instrument) that modulates the voltage bias at a frequency $f = 599$ Hz with an amplitude of ~ 20 mV.

2. STM topographies of typical defects on graphite surface.

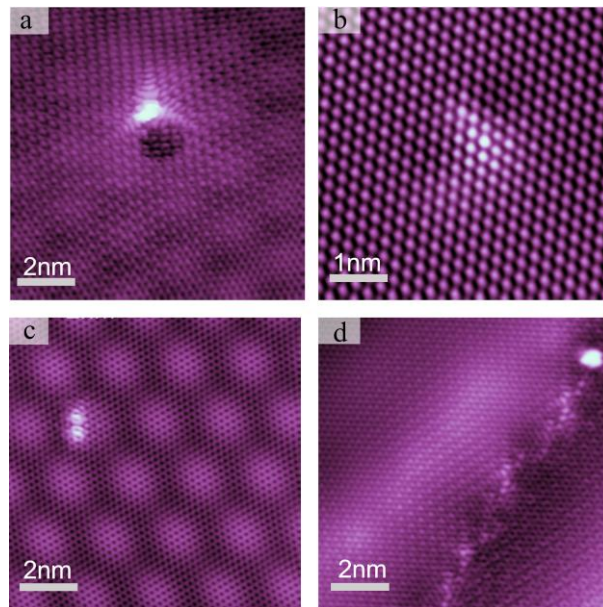


Figure S1. STM topographies of typical defects in natural graphite. a) single vacancy, b) heteroatom replacement. c, d) heterocycle located in a moiré region and grain boundary, pentagon-heptagon and pentagon-octagon defects are usually found in newly cleaved HOPG surface or grown graphene with low crystallinity. Scanning parameters: a) 100 mV, 900 pA; b) 30 mV, 100 pA; c) 100 mV, 300 pA; and d) 200 mV, 10 pA.

3. Superstructure domain discrimination.

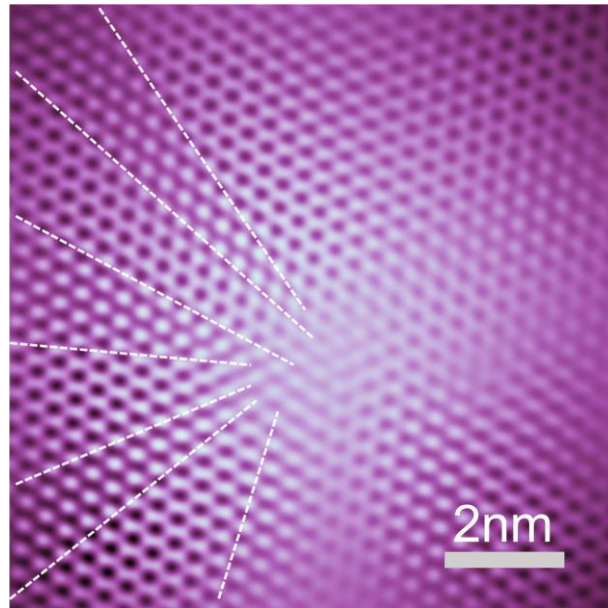


Figure S2. FFT filtered image of figure 1a, the honeycomb and single bright atom can be easily distinguished, corresponding to the honeycomb and $(\sqrt{3} \times \sqrt{3}) R30^\circ$ superstructure, respectively.

4. Additional STS measured along the GB.

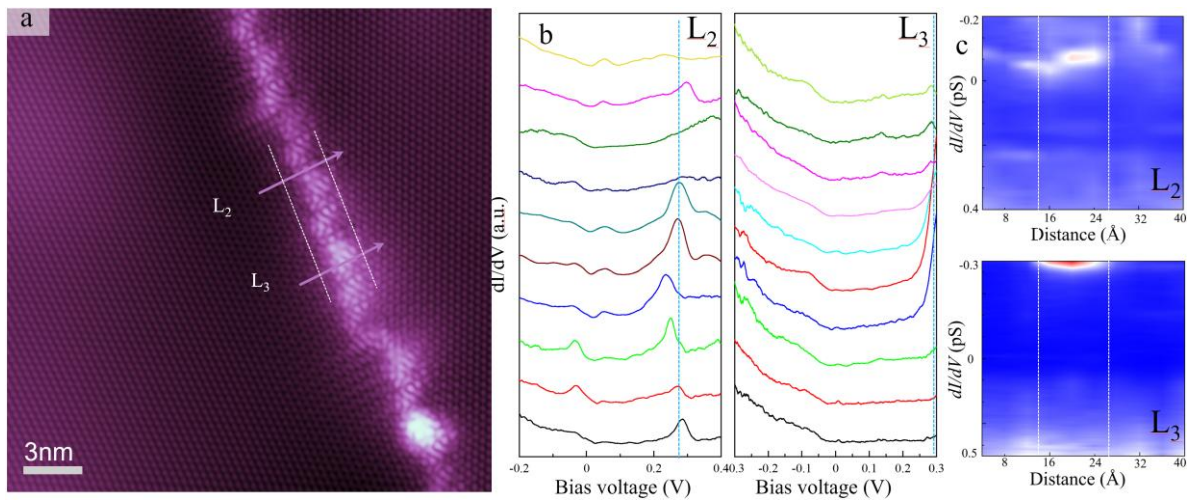


Figure S3. a) dI/dV curves taken across the boundary labeled as L_2 and L_3 , the corresponding line mappings are show in figure c. Localized electronic states emerge at ~ 0.24 V and 0.3 V, as marked by light blue dashed line in b, the states have the same spatial distribution with the length of the GB.

5. Electron wave scattering behavior caused by the GB.

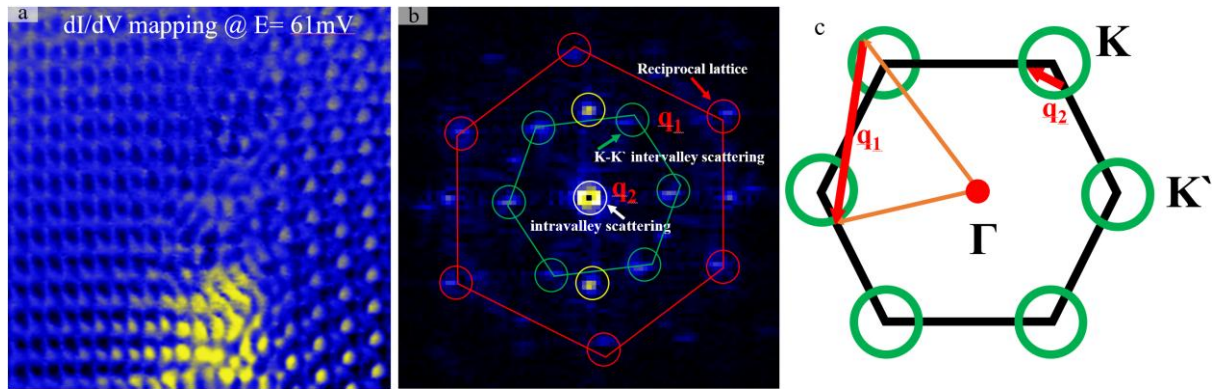


Figure S4. a) dI/dV mapping at 61 mV. b) FFT-STs map of figure a, the spot marked by red circles arise from surface graphene lattice, the intervalley scattering related spots are denoted with green circles, the center bright region indicates the intravalley related scatterings. Possible scattering channels are denoted by yellow circles in FFT-STs. c) Schematic of the 2D Brillouin zone (black lines), constant energy contours (green rings) at the K-K' points, and the two dominant classes of scattering vectors that create the interference patterns.

6. Decay length extraction.

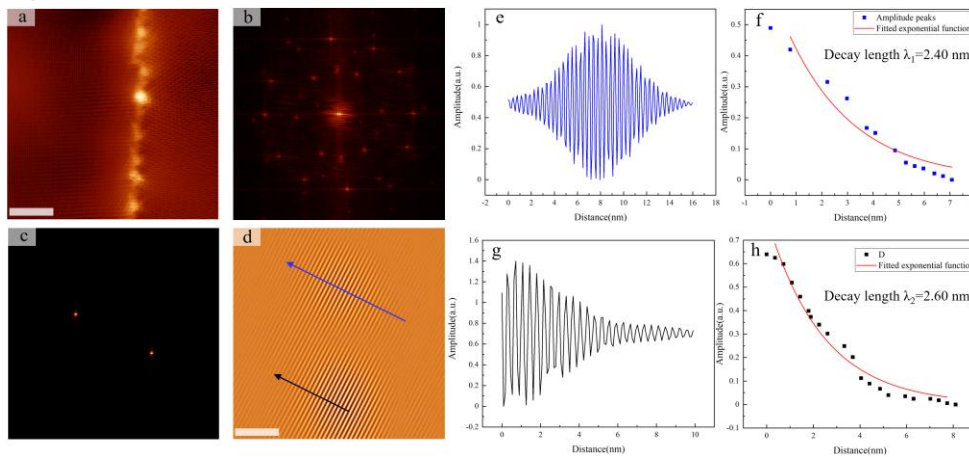


Figure S5. a, b) STM topography of GB and the corresponding Fast Fourier transform (FFT) pattern. c,d) two picked spot and its inversed real space pattern. Two line across the scattering pattern are indicated in d) with their line profiles showing in e and g, the interference propagates into the bulk with decreasing intensity and clear long-range oscillations in e and g. f, h) The corresponding peak intensities and fitted exponential decay function of e and g, giving decay length of 2.40 and 2.60 nm of selected scattering channel. Scale bar: 4 nm.